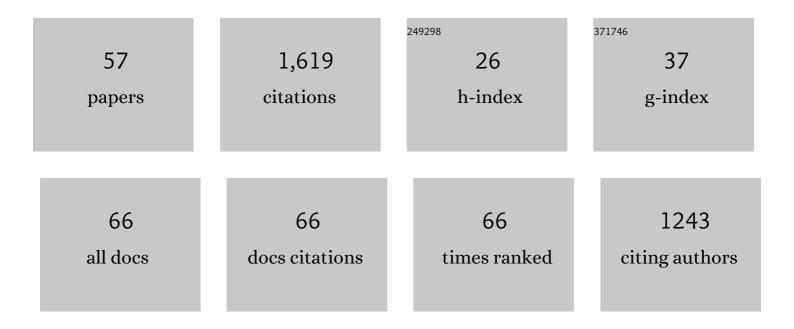
## Tomoko Matsuo

List of Publications by Year in descending order

Source: https://exaly.com/author-pdf/3714269/publications.pdf Version: 2024-02-01



#	Article	IF	CITATIONS
1	Assimilative Mapping of Auroral Electron Energy Flux Using SSUSI Lymanâ€Birgeâ€Hopfield (LBH) Emissions. Journal of Geophysical Research: Space Physics, 2022, 127, .	0.8	1
2	Retrospect and prospect of ionospheric weather observed by FORMOSAT-3/COSMIC and FORMOSAT-7/COSMIC-2. Terrestrial, Atmospheric and Oceanic Sciences, 2022, 33, .	0.3	5
3	Extreme Positive Ionosphere Storm Triggered by a Minor Magnetic Storm in Deep Solar Minimum Revealed by FORMOSATâ€7/COSMICâ€2 and GNSS Observations. Journal of Geophysical Research: Space Physics, 2021, 126, e2020JA028261.	0.8	21
4	Dataâ€Ðriven Ensemble Modeling of Equatorial Ionospheric Electrodynamics: A Case Study During a Minor Storm Period Under Solar Minimum Conditions. Journal of Geophysical Research: Space Physics, 2021, 126, e2020JA028539.	0.8	4
5	Multiresolution Modeling of High‣atitude Ionospheric Electric Field Variability and Impact on Joule Heating Using SuperDARN Data. Journal of Geophysical Research: Space Physics, 2021, 126, e2021JA029196.	0.8	4
6	Deriving column-integrated thermospheric temperature with the N <sub>2</sub> Lyman–Birge–HopfieldÂ(2,0) band. Atmospheric Measurement Techniques, 2021, 14, 6917-6928.	1.2	0
7	Localâ€Time and Vertical Characteristics of Quasiâ€6â€Day Oscillation in the Ionosphere During the 2019 Antarctic Sudden Stratospheric Warming. Geophysical Research Letters, 2020, 47, e2020GL090345.	1.5	30
8	The Early Results and Validation of FORMOSATâ€7/COSMICâ€2 Space Weather Products: Global Ionospheric Specification and Neâ€Aided Abel Electron Density Profile. Journal of Geophysical Research: Space Physics, 2020, 125, e2020JA028028.	0.8	47
9	Event Studies of High‣atitude FACs With Inverse and Assimilative Analysis of AMPERE Magnetometer Data. Journal of Geophysical Research: Space Physics, 2020, 125, e2019JA027266.	0.8	3
10	Modes of (FACs) Variability and Their Hemispheric Asymmetry Revealed by Inverse and Assimilative Analysis of Iridium Magnetometer Data. Journal of Geophysical Research: Space Physics, 2020, 125, e2019JA027265.	0.8	13
11	Recent Progress on Inverse and Data Assimilation Procedure for High-Latitude Ionospheric Electrodynamics. , 2020, , 219-232.		9
12	Ionospheric responses to the 21 August 2017 solar eclipse by using data assimilation approach. Progress in Earth and Planetary Science, 2019, 6, .	1.1	23
13	Upper Atmosphere Radiance Data Assimilation: A Feasibility Study for GOLD Far Ultraviolet Observations. Journal of Geophysical Research: Space Physics, 2019, 124, 8154-8164.	0.8	9
14	Revisiting the Modulations of Ionospheric Solar and Lunar Migrating Tides During the 2009 Stratospheric Sudden Warming by Using Global Ionosphere Specification. Space Weather, 2019, 17, 767-777.	1.3	20
15	Effects of Nearly Frontal and Highly Inclined Interplanetary Shocks on Highâ€Latitude Fieldâ€Aligned Currents (FACs). Space Weather, 2019, 17, 1659-1673.	1.3	9
16	Spaceâ€Based Sentinels for Measurement of Infrared Cooling in the Thermosphere for Space Weather Nowcasting and Forecasting. Space Weather, 2018, 16, 363-375.	1.3	20
17	A multi-resolution model for non-Gaussian random fields on a sphere with application to ionospheric electrostatic potentials. Annals of Applied Statistics, 2018, 12, 459-489.	0.5	5
18	Modeling Tangential Vector Fields on a Sphere. Journal of the American Statistical Association, 2018, 113, 1625-1636.	1.8	13

Томоко Матѕио

#	Article	IF	CITATIONS
19	Impact of Assimilating the FORMOSATâ€3/COSMIC and FORMOSATâ€7/COSMICâ€2 RO Data on the Midlatitude and Lowâ€Latitude Ionospheric Specification. Earth and Space Science, 2018, 5, 875-890.	1.1	23
20	Understanding the Global Variability in Thermospheric Nitric Oxide Flux Using Empirical Orthogonal Functions (EOFs). Journal of Geophysical Research: Space Physics, 2018, 123, 4150-4170.	0.8	20
21	Quantifying the Sources of Ionosphere Dayâ€Toâ€Day Variability. Journal of Geophysical Research: Space Physics, 2018, 123, 9682-9696.	0.8	38
22	Assessment of the Impact of FORMOSATâ€7/COSMICâ€2 GNSS RO Observations on Midlatitude and Lowâ€Latitude Ionosphere Specification: Observing System Simulation Experiments Using Ensemble Square Root Filter. Journal of Geophysical Research: Space Physics, 2018, 123, 2296-2314.	0.8	32
23	On the Dynamical Control of the Mesosphere–Lower Thermosphere by the Lower and Middle Atmosphere. Journals of the Atmospheric Sciences, 2017, 74, 933-947.	0.6	58
24	Modeling the ionospheric prereversal enhancement by using coupled thermosphereâ€ionosphere data assimilation. Geophysical Research Letters, 2017, 44, 1652-1659.	1.5	32
25	Data Assimilation of Groundâ€Based GPS and Radio Occultation Total Electron Content for Global Ionospheric Specification. Journal of Geophysical Research: Space Physics, 2017, 122, 10,876.	0.8	33
26	Equatorial plasma bubble generation/inhibition during 2015ÂSt. Patrick's Day storm. Space Weather, 2017, 15, 1141-1150.	1.3	16
27	Ushering in a New Frontier in Geospace Through Data Science. Journal of Geophysical Research: Space Physics, 2017, 122, 12,586.	0.8	28
28	lonosphere data assimilation modeling of 2015 St. Patrick's Day geomagnetic storm. Journal of Geophysical Research: Space Physics, 2016, 121, 11,549.	0.8	23
29	Highâ€latitude ionospheric conductivity variability in three dimensions. Geophysical Research Letters, 2016, 43, 7867-7877.	1.5	14
30	Optimal interpolation analysis of highâ€latitude ionospheric Hall and Pedersen conductivities: Application to assimilative ionospheric electrodynamics reconstruction. Journal of Geophysical Research: Space Physics, 2016, 121, 4898-4923.	0.8	32
31	Ionospheric data assimilation with thermosphereâ€ionosphereâ€electrodynamics general circulation model and GPSâ€TEC during geomagnetic storm conditions. Journal of Geophysical Research: Space Physics, 2016, 121, 5708-5722.	0.8	40
32	Ionospheric data assimilation and forecasting during storms. Journal of Geophysical Research: Space Physics, 2016, 121, 764-778.	0.8	51
33	Mapping highâ€latitude ionospheric electrodynamics with SuperDARN and AMPERE. Journal of Geophysical Research: Space Physics, 2015, 120, 5854-5870.	0.8	38
34	Dominant modes of variability in largeâ€scale Birkeland currents. Journal of Geophysical Research: Space Physics, 2015, 120, 6722-6735.	0.8	22
35	Modes of highâ€latitude auroral conductance variability derived from DMSP energetic electron precipitation observations: Empirical orthogonal function analysis. Journal of Geophysical Research: Space Physics, 2015, 120, 11,013.	0.8	37
36	Inverse procedure for highâ€latitude ionospheric electrodynamics: Analysis of satelliteâ€borne magnetometer data. Journal of Geophysical Research: Space Physics, 2015, 120, 5241-5251.	0.8	22

Томоко Матѕио

#	Article	IF	CITATIONS
37	lonospheric assimilation of radio occultation and ground-based GPS data using non-stationary background model error covariance. Atmospheric Measurement Techniques, 2015, 8, 171-182.	1.2	49
38	Fieldâ€aligned neutral wind bias correction scheme for global ionospheric modeling at midlatitudes by assimilating FORMOSATâ€3/COSMIC <i><scp><i>h<sub>m</sub>F</i></scp></i> 2 data under geomagnetically quiet conditions. Journal of Geophysical Research: Space Physics, 2015, 120, 3130-3149.	0.8	21
39	Effects of inferring unobserved thermospheric and ionospheric state variables by using an Ensemble Kalman Filter on global ionospheric specification and forecasting. Journal of Geophysical Research: Space Physics, 2014, 119, 9256-9267.	0.8	43
40	Comparison of magnetic perturbation data from LEO satellite constellations: Statistics of DMSP and AMPERE. Space Weather, 2014, 12, 2-23.	1.3	33
41	SuperDARN assimilative mapping. Journal of Geophysical Research: Space Physics, 2013, 118, 7954-7962.	0.8	33
42	Groundâ€based GPS observation of SEDâ€associated irregularities over CONUS. Journal of Geophysical Research: Space Physics, 2013, 118, 2478-2489.	0.8	18
43	Thermospheric mass density specification using an ensemble Kalman filter. Journal of Geophysical Research: Space Physics, 2013, 118, 1339-1350.	0.8	53
44	Modeling impact of FORMOSATâ€7/COSMICâ€2 mission on ionospheric space weather monitoring. Journal of Geophysical Research: Space Physics, 2013, 118, 6518-6523.	0.8	23
45	Mesoscale and largeâ€scale variability in highâ€ŀatitude ionospheric convection: Dominant modes and spatial/temporal coherence. Journal of Geophysical Research: Space Physics, 2013, 118, 7895-7904.	0.8	25
46	Assimilation of FORMOSATâ€3/COSMIC electron density profiles into a coupled thermosphere/ionosphere model using ensemble Kalman filtering. Journal of Geophysical Research, 2012, 117, .	3.3	74
47	Annual and semiannual variations of thermospheric density: EOF analysis of CHAMP and GRACE data. Journal of Geophysical Research, 2012, 117, .	3.3	55
48	A realâ€ŧime run of the Coupled Thermosphere Ionosphere Plasmasphere Electrodynamics (CTIPe) model. Space Weather, 2012, 10, .	1.3	61
49	Data assimilation of thermospheric mass density. Space Weather, 2012, 10, .	1.3	41
50	Role of thermosphereâ€ionosphere coupling in a global ionospheric specification. Radio Science, 2011, 46, .	0.8	35
51	Nonstationary covariance modeling for incomplete data: Monte Carlo EM approach. Computational Statistics and Data Analysis, 2011, 55, 2059-2073.	0.7	18
52	Principal modes of thermospheric density variability: Empirical orthogonal function analysis of CHAMP 2001–2008 data. Journal of Geophysical Research, 2010, 115, .	3.3	38
53	Effects of highâ€latitude ionospheric electric field variability on global thermospheric Joule heating and mechanical energy transfer rate. Journal of Geophysical Research, 2008, 113, .	3.3	57
54	Towards understanding the electrodynamics of the 3-dimensional high-latitude ionosphere: present and future. Annales Geophysicae, 2008, 26, 3913-3932.	0.6	22

#	Article	IF	CITATIONS
55	Optimal interpolation analysis of high-latitude ionospheric electrodynamics using empirical orthogonal functions: Estimation of dominant modes of variability and temporal scales of large-scale electric fields. Journal of Geophysical Research, 2005, 110, .	3.3	45
56	Modes of high-latitude electric field variability derived from DE-2 measurements: Empirical Orthogonal Function (EOF) analysis. Geophysical Research Letters, 2002, 29, 11-1.	1.5	56
57	Modeling thermospheric neutral density waves and holes in response to high latitude forcing. Advances in Space Research, 1999, 24, 1447-1458.	1.2	14